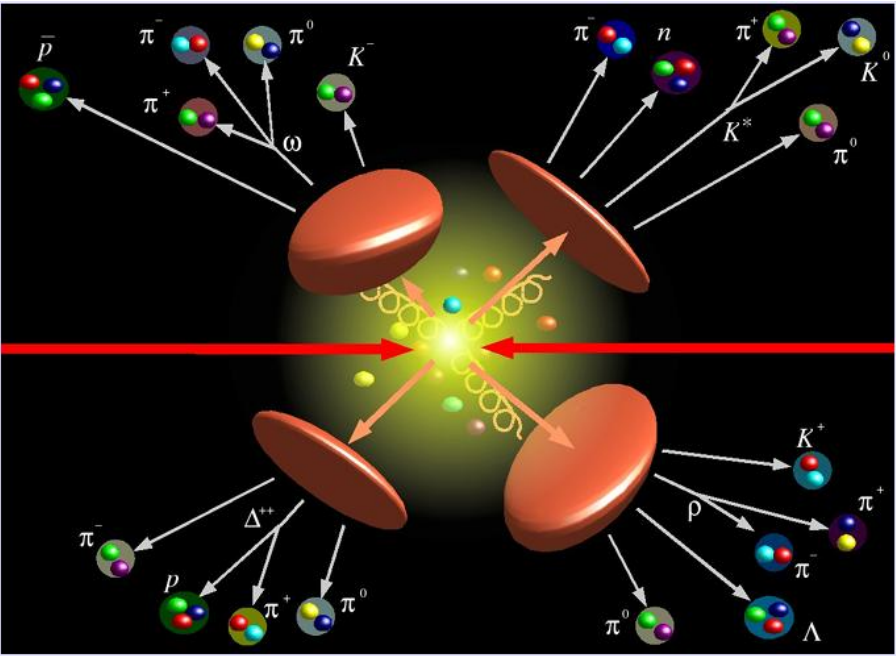
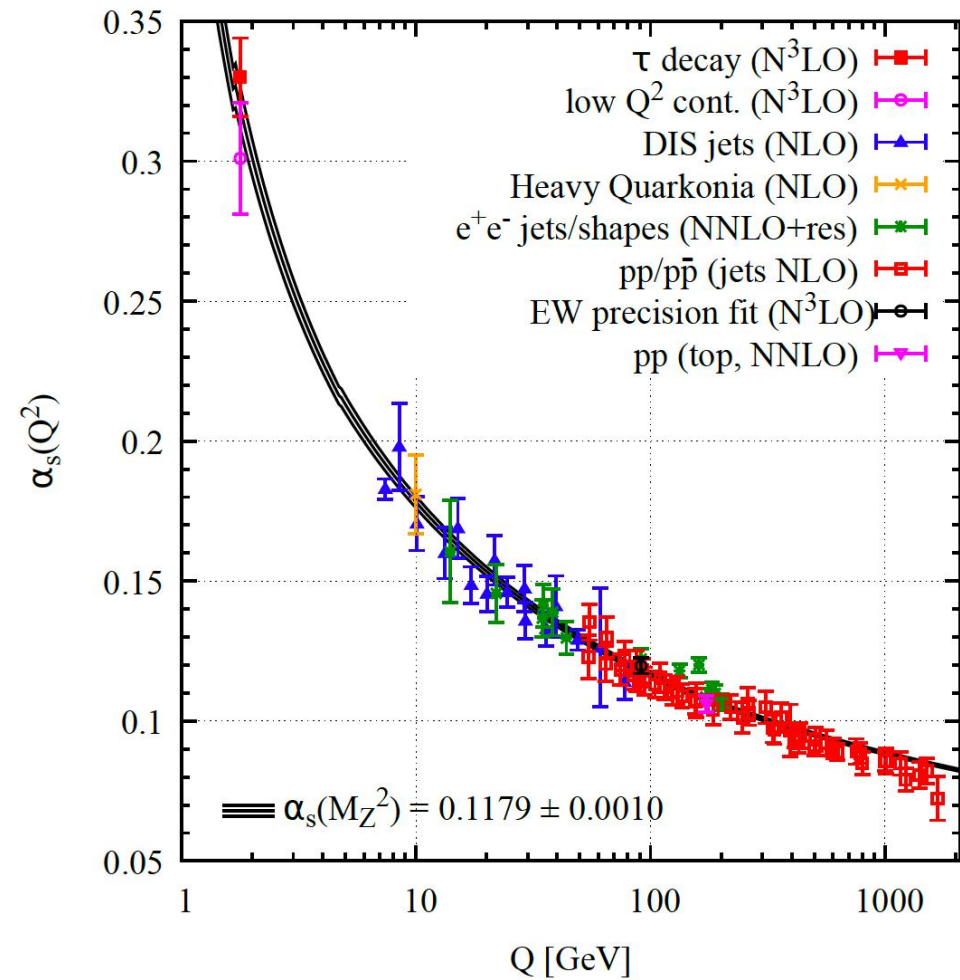
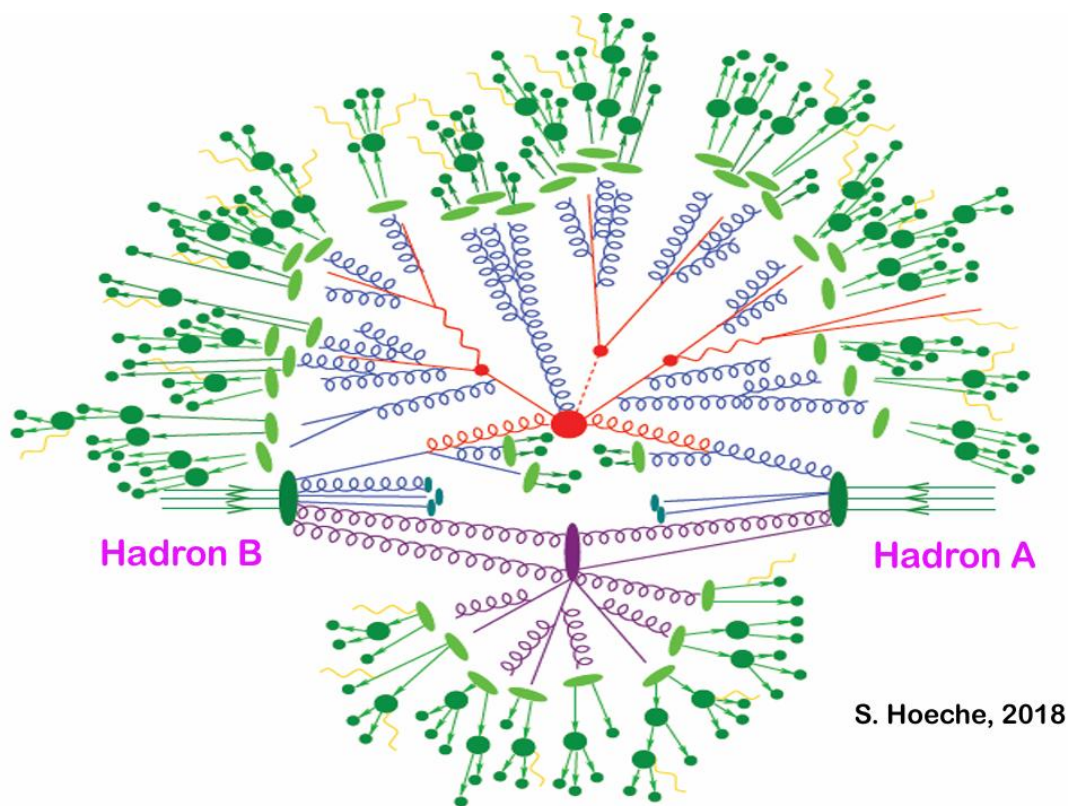


An introduction to the introduction to the Statistical Hadronization Model

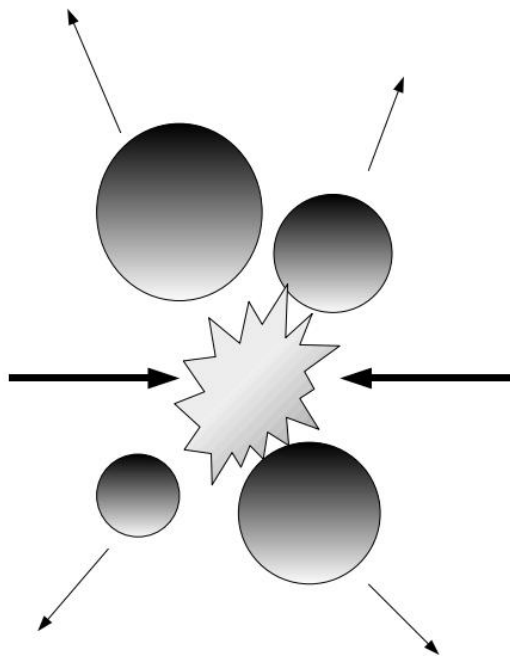


Jingyu Zhang

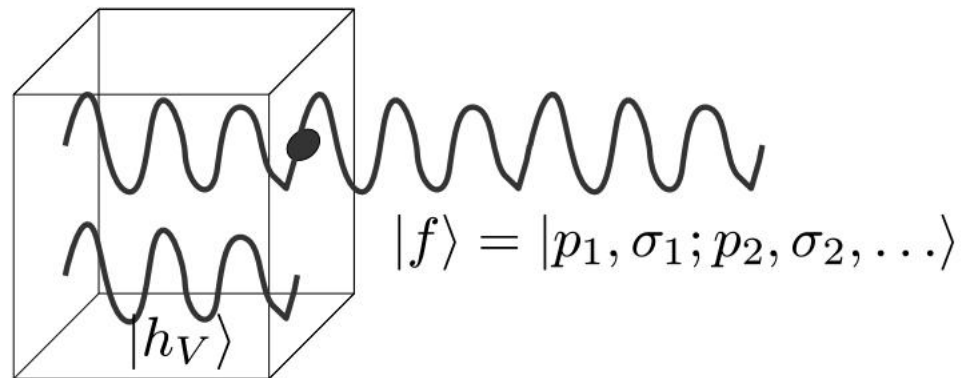
Hadronization



Cluster



$\mathbf{Q} = (Q, B, S, \dots)$
 $M = \text{mass}$
 $J, \lambda = \text{spin, 3}^{\text{rd}} \text{ comp.}$
 $V = \text{volume}$
 Isospin, parity, C-parity



$$|f\rangle = |p_1, \sigma_1, \dots, p_N, \sigma_N\rangle \quad (1)$$

$$|N\rangle_V = \alpha_{0,N} |0\rangle + \alpha_{1,N} |1\rangle + \dots + \alpha_{N,N} |N\rangle + \dots \quad (2)$$

The formalism: basics

$$\rho \propto \sum_{h_V} P_i |h_V\rangle \langle h_V| P_i \equiv P_i P_V P_i \quad (3)$$

$$P_i = P_{P,J,\lambda,\pi} P_{inner} \quad (4)$$

$$P_{P,J,\lambda,\pi} = \delta^4(P - \hat{P}) P_{J,\lambda} \frac{I + \pi \hat{\Pi}}{2} \quad (5)$$

$$P_{inner} = P_{I,I_3} P_Q P_\chi \quad (6)$$

$$p_f \propto \langle f | P_i P_V P_i | f \rangle \quad (7)$$

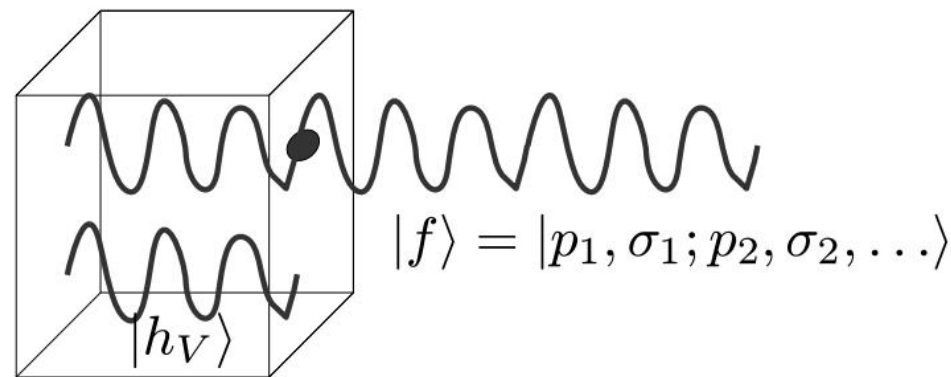
$$\sum_f p_f \propto \text{tr}(P_i P_V P_i) = \text{tr}(P_i^2 P_V) = \text{atr}(P_i P_V) \quad (8)$$

$$\text{tr}(P_i P_V) = \sum_{h_V} \langle h_V | P_i | h_V \rangle \equiv \Omega \quad (9)$$

$$\Omega = \sum_{h_V} \langle h_V | \delta^4(P - \hat{P}) | h_V \rangle \quad (10)$$

$$|\psi\rangle = \sum_{h_V} c_{h_V} P_i |h_V\rangle \quad \text{with } |c_{h_V}|^2 = \text{const}. \quad (11)$$

$$\begin{aligned} |\langle f | \psi \rangle|^2 &= \left| \sum_{h_V} \langle f | P_i | h_V \rangle c_{h_V} \right|^2 \\ &= \text{const} \sum_{h_V} |\langle f | P_i | h_V \rangle|^2 + \sum_{h_V \neq h'_V} \langle f | P_i | h_V \rangle \langle h'_V | P_i | f \rangle c_{h_V} c_{h'_V}^* \end{aligned} \quad (12)$$



Rates of multiparticle channels

$$\Omega_{\{N_j\}} = \frac{V^N}{(2\pi)^{3N}} \left(\prod_{j=1}^K (2S_j + 1)^{N_j} \frac{1}{N_j!} \right) \int d^3 p_1 \dots \int d^3 p_N \delta^4(P_0 - \sum_i p_i) \langle 0|P_V|0\rangle \quad \text{a four-volume } \underline{\Upsilon} = Vu \quad (14)$$

$$\Omega_{\{N_j\}} = \frac{1}{(2\pi)^{3N}} \left(\prod_{j=1}^K (2S_j + 1)^{N_j} \frac{1}{N_j!} \right) \int d^4 p_1 \dots \int d^4 p_N \left[\prod_{i=1}^N \Upsilon \cdot p_i \delta(p_i^2 - m_i^2) \theta(p_i^0) \right] \delta^4(P_0 - \sum_i p_i) \langle 0|P_V|0\rangle \quad (15)$$

$$\Gamma_N \propto \sum_{\sigma_1, \dots, \sigma_N} \frac{1}{(2\pi)^{3N}} \left(\prod_{j=1}^K \frac{1}{N_j!} \right) \int d^3 p_1/2\epsilon_1 \dots \int d^3 p_N/2\epsilon_N |M_{fi}|^2 \delta^4(P_0 - \sum_i p_i) \quad (16)$$

$$\begin{array}{c} \downarrow \\ |M_{fi}|^2 \propto \prod_{i=1}^N \Upsilon \cdot p_i \end{array} \quad (17) \quad \longrightarrow \quad |M_{fi}|^2 \propto \frac{1}{\rho^N} \prod_{i=1}^N P \cdot p_i. \quad (18)$$

This expression explicitly shows the separation between the kinematic arguments of the dynamical matrix element, and the scale $1/\rho$ which determines particle production. This ought to be ultimately related to the fundamental scale of quantum chromodynamics, Λ_{QCD} .

Rates of multiparticle channels

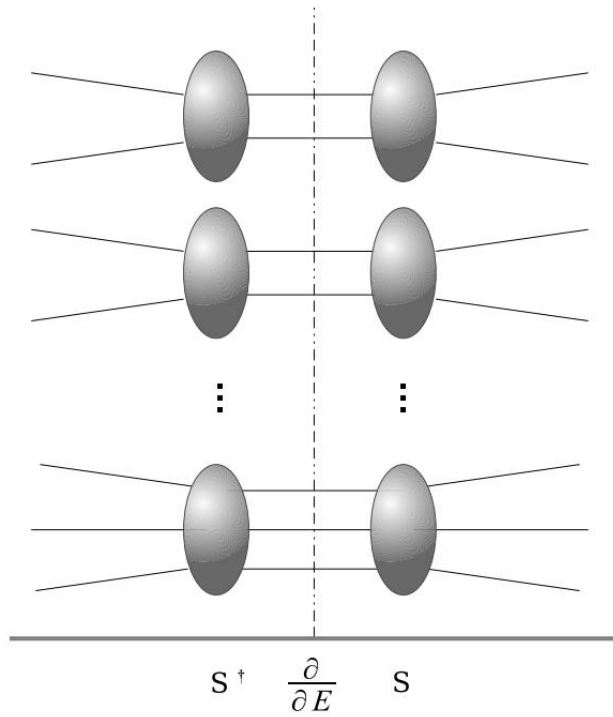
The finite cluster size is the distinctive feature of the SHM:

$$\Omega_{\{N_j\}} = \int d^3p_1 \dots d^3p_N \delta^4(P_0 - \sum_{i=1}^N p_i) \prod_j \sum_{\{h_{n_j}\}} \frac{(\mp 1)^{N_j+H_j} (2S_j + 1)^{H_j}}{\prod_{n_j=1}^{N_j} n_j^{h_{n_j}} h_{n_j}!} \quad (19)$$

$$\times \prod_{l_j=1}^{H_j} F_{n_{l_j}} \langle 0 | P_V | 0 \rangle$$

$$F_{n_l} = \prod_{i_l=1}^{n_l} \frac{1}{(2\pi)^3} \int_V d^3x e^{i\mathbf{x} \cdot (\mathbf{p}_{c_l(i_l)} - \mathbf{p}_{i_l})} \quad (20)$$

Interactions



$$\sum_f p_f \propto \text{tr}(\mathbf{P}_i \mathbf{P}_V \mathbf{P}_i) = a \text{tr}(\mathbf{P}_i \mathbf{P}_V) = a \sum_{h_V} \langle h_V | \mathbf{P}_i | h_V \rangle \equiv a \Omega \quad (21)$$

$$\text{tr} \delta^4(P - \hat{P}) = \text{tr} \delta^4(P - \hat{P}_0) + \frac{1}{4\pi i} \text{tr} \left[\delta^4(P - \hat{P}_0) \hat{\mathcal{S}}^{-1} \overleftrightarrow{\frac{\partial}{\partial E}} \hat{\mathcal{S}} \right] \quad (22)$$

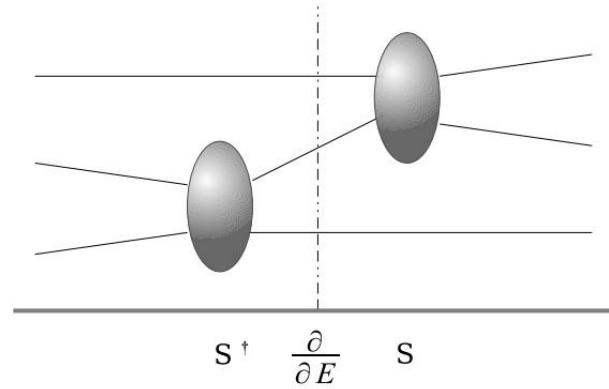


Figure 3: Left panel: symmetric diagrams for the cluster decomposition of the interaction term in the DMB theorem. Right panel: non-symmetric diagrams.

High energy collisions

$$\langle n_j \rangle^{\text{primary}} = \frac{VT(2S_j + 1)}{2\pi^2} \sum_{n=1}^{\infty} \gamma_s^{N_s n} (\mp 1)^{n+1} \frac{m_j^2}{n} K_2 \left(\frac{nm_j}{T} \right) \frac{Z(\mathbf{Q} - n\mathbf{q}_j)}{Z(\mathbf{Q})} \quad (23)$$

$$\langle n_j \rangle = \langle n_i \rangle^{\text{primary}} + \sum_k \text{Br}(k \rightarrow j) \langle n_k \rangle. \quad (24)$$

$$Z(\mathbf{Q}) = \frac{1}{(2\pi)^N} \int_{-\pi}^{+\pi} d^N \phi e^{i\mathbf{Q} \cdot \phi} \\ \times \exp \left[\frac{V}{(2\pi)^3} \sum_j (2S_j + 1) \int d^3 p \log (1 \pm \gamma_s^{N_s j} e^{-\sqrt{p^2 + m_j^2}/T_i - i\mathbf{q}_j \cdot \phi})^{\pm 1} \right] \quad (25)$$

High energy collisions

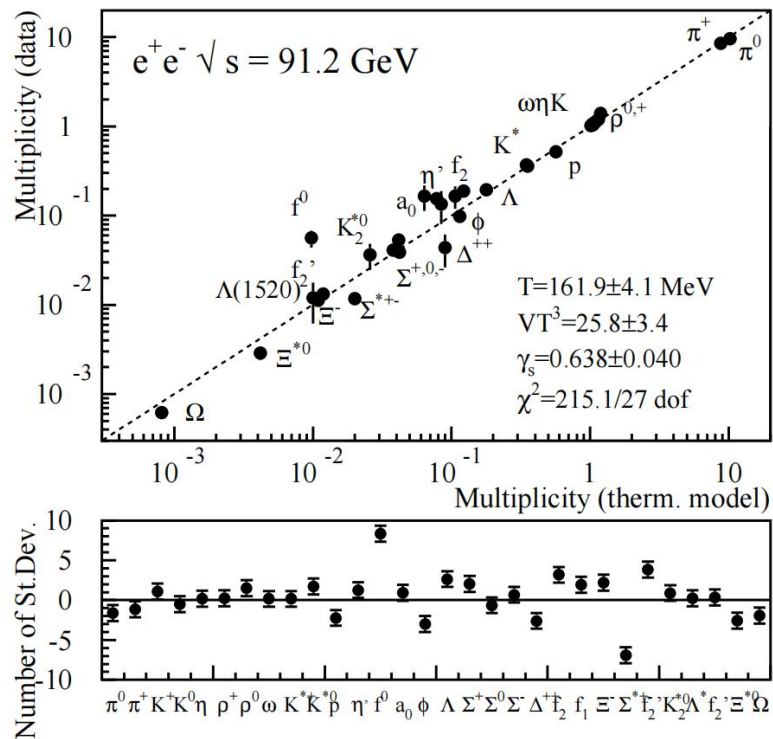


Figure 4: Upper panel: measured vs theoretical multiplicities of light-flavoured hadrons in e^+e^- collisions at $\sqrt{s} = 91.25 \text{ GeV}$. Lower panel: fit residuals (from ref. [17]).

Particle	Experiment (E)	Model (M)	Residual	$(M - E)/E$ [%]
D^0	0.559 ± 0.022	0.5406	-0.83	-3.2
D^+	0.238 ± 0.024	0.2235	-0.60	-6.1
D^{*+}	0.2377 ± 0.0098	0.2279	-1.00	-4.1
D^{*0}	0.218 ± 0.071	0.2311	0.18	6.0
D_1^0	0.0173 ± 0.0039	0.01830	0.26	5.8
D_2^{*0}	0.0484 ± 0.0080	0.02489	-2.94	-48.6
D_s	0.116 ± 0.036	0.1162	0.006	0.19
D_s^*	0.069 ± 0.026	0.0674	-0.06	-2.4
D_{s1}	0.0106 ± 0.0025	0.00575	-1.94	-45.7
D_{s2}^*	0.0140 ± 0.0062	0.00778	-1.00	-44.5
Λ_c	0.079 ± 0.022	0.0966	0.80	22.2
$(B^0 + B^+)/2$	0.399 ± 0.011	0.3971	-0.18	-0.49
B_s	0.098 ± 0.012	0.1084	0.87	10.6
$B^*/B(\text{uds})$	0.749 ± 0.040	0.6943	-1.37	-7.3
$B^{**} \times BR(B^{*})\pi$	0.180 ± 0.025	0.1319	-1.92	-26.7
$(B_2^* + B_1) \times BR(B^{*})\pi$	0.090 ± 0.018	0.0800	-0.57	-11.4
$B_{s2}^* \times BR(BK)$	0.0093 ± 0.0024	0.00631	-1.24	-32.1
b-baryon	0.103 ± 0.018	0.09751	-0.30	-5.3
Ξ_b^-	0.011 ± 0.006	0.00944	-0.26	-14.2

Table 1: Abundances of charmed hadrons in $e^+e^- \rightarrow c\bar{c}$ annihilations and bottomed hadrons in $e^+e^- \rightarrow b\bar{b}$ annihilations at $\sqrt{s} = 91.25 \text{ GeV}$, compared to the prediction of the statistical model (from ref. [17]).

High energy collisions

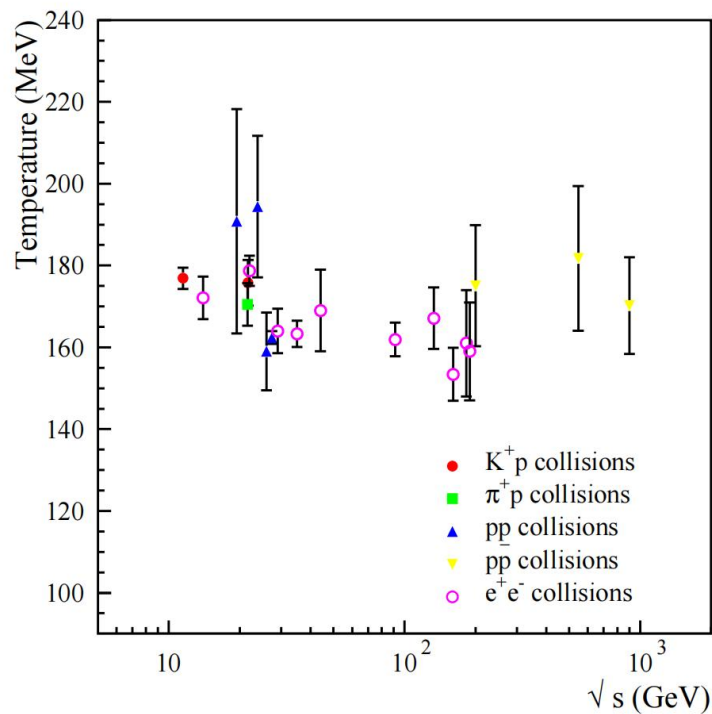


Figure 5: Temperatures fitted in elementary collisions as a function of center-of-mass energy.

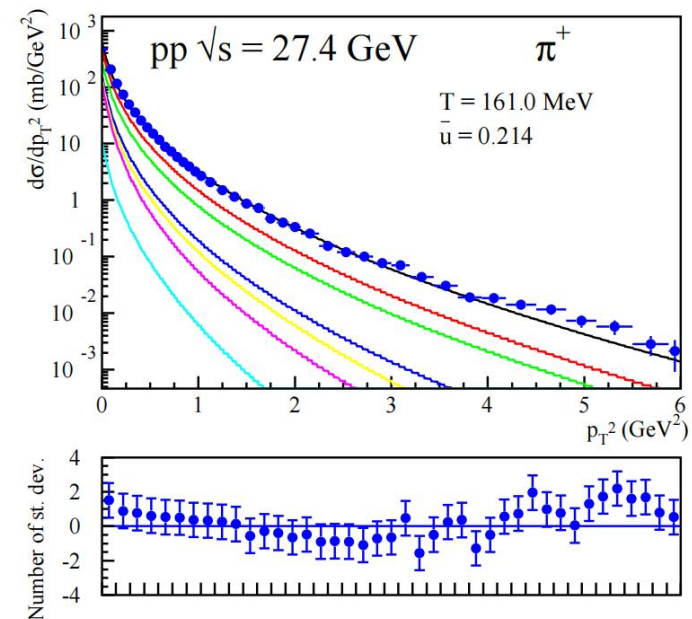


Figure 6: Transverse momentum spectrum of π^+ in pp collisions at $\sqrt{s} = 27$ GeV (from ref. [16]). Full dots are data from experiment NA27; the black line is a fit with temperature $T=161$ MeV and average transverse four-velocity of hadronizing clusters ~ 0.21 . Coloured lines show the cumulative contribution of resonance decays, divided into classes according to their quantum numbers.

Heavy ion collisions

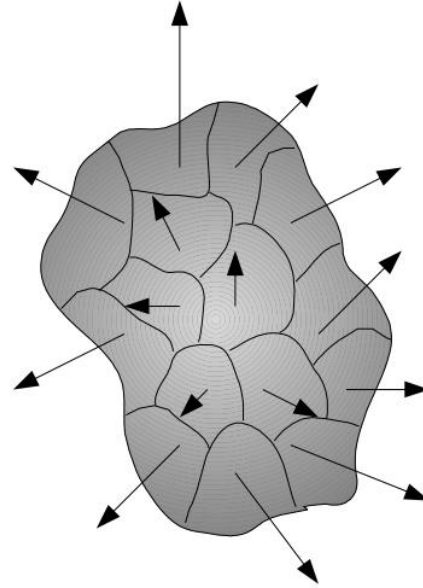


Figure 7: Spatial distributions of clusters in heavy ion collisions according to the hydrodynamical picture. In this model, nearby clusters interact from an early stage on and their momenta and charges are strongly correlated with their positions, unlike in elementary collisions.

$$\langle n_j \rangle_{\text{primary}} = \frac{VT(2S_j + 1)}{2\pi^2} \sum_{n=1}^{\infty} \gamma_S^{N_s n} (\mp 1)^{n+1} \frac{m_j^2}{n} K_2 \left(\frac{nm_j}{T} \right) \exp[n\boldsymbol{\mu} \cdot \mathbf{q}_j/T]. \quad (26)$$

Heavy ion collisions

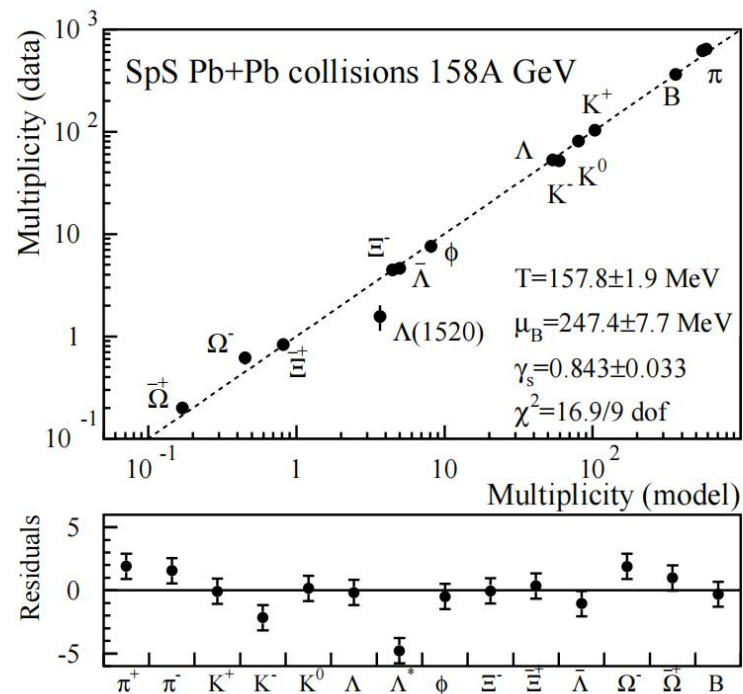
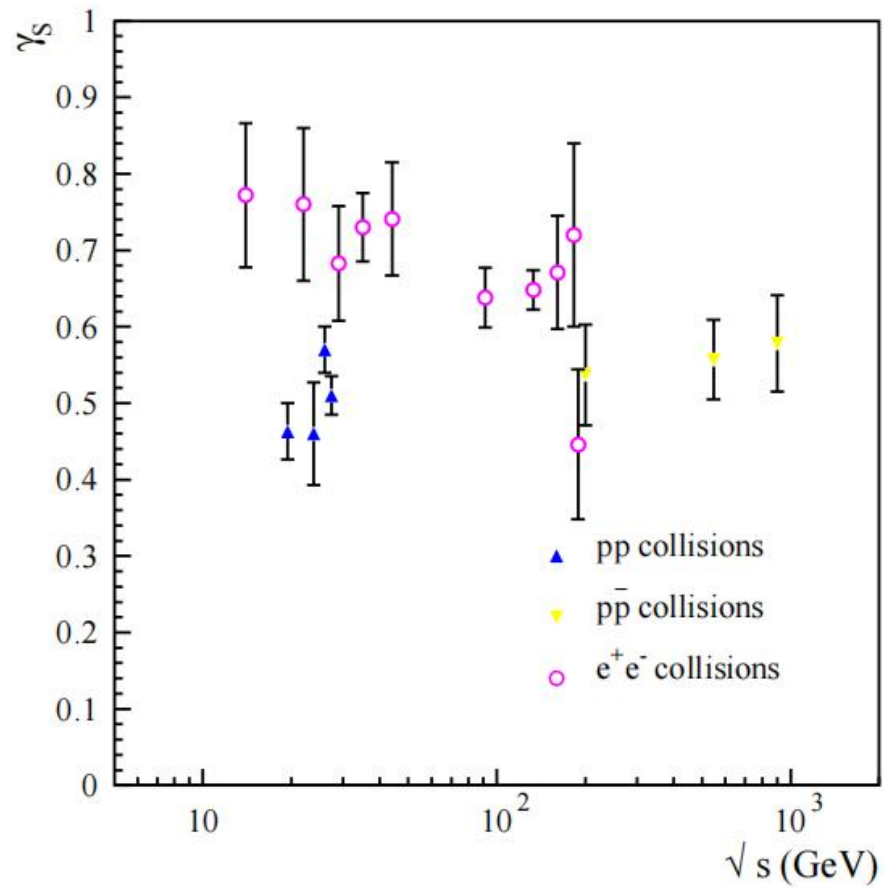
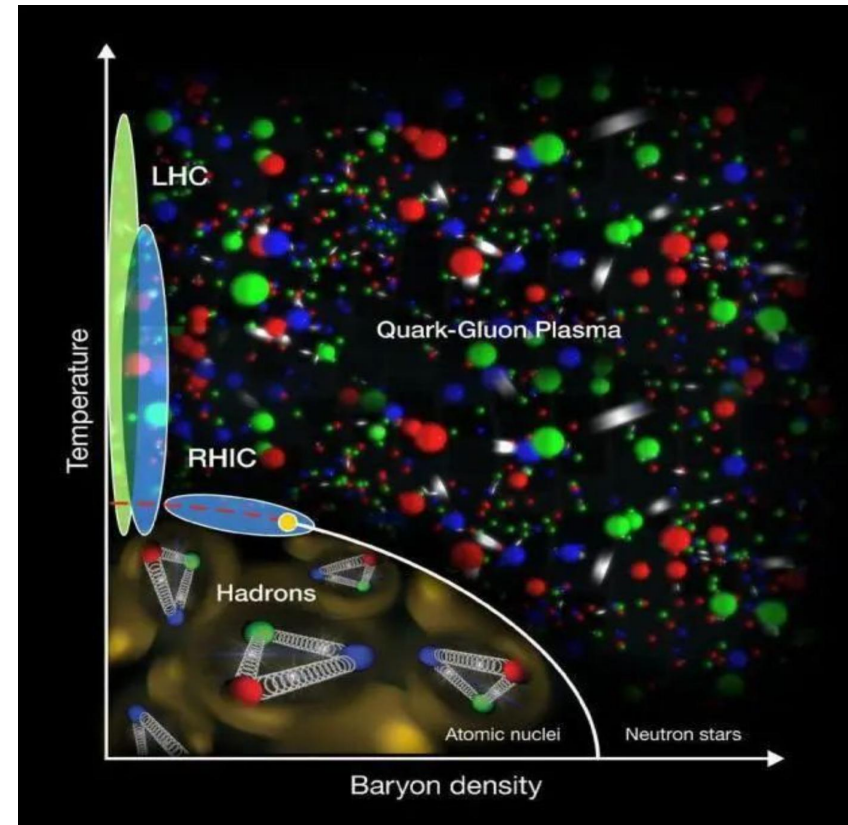


Figure 8: Upper panel: measured vs theoretical multiplicities of light-flavoured hadrons in Pb-Pb collisions at $\sqrt{s_{NN}} = 17.2$ GeV. Lower panel: fit residuals (from ref. [21]).

Parameters on SHM

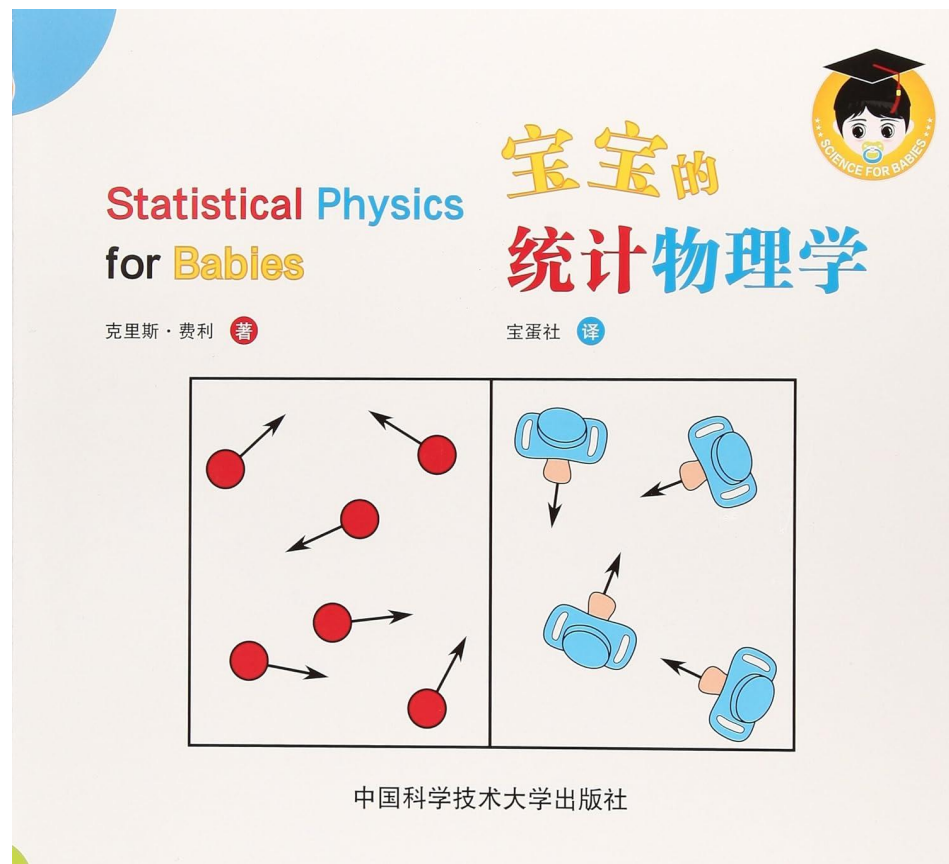


$$\gamma_S < 1$$



$$T \approx 160 \text{ MeV}$$

Thermalization: how is it achieved?



- 基本粒子碰撞中，强子间的二体碰撞无法实现热化，因为膨胀速率较快，强子之间的相互作用时间不够长。
- 在重离子碰撞中，数据中的某些特征不能通过强子动力学模型来解释，这表明需要考虑多体碰撞。
- 一种新的解释是将禁闭现象与黑洞物理进行类比，认为强子化过程中的温度类似于霍金辐射。
- 这种理论认为温度与弦张力相关，并且是普遍的。

Summary

- cluster definition
- review the basic formula on SHM
- consider infinite volume and interaction
- compare with experiments (hadron production on ee, pp, heavy ion)
- parameters discussion
- Thermalization

THANKS FOR YOUR ATTENTION